Available online at www.sciencedirect.com
ScienceDirect
Optical Materials 30 (2008) 1747–1754
OPTICAL Materials
www.elsevier.com/locate/optmat

Absolute Raman cross-sections of some explosives: Trend to UV

L. Nagli [a,b], M. Gaft [a], Y. Fleger [c], M. Rosenbluh [c,*]

[a] Laser Detect Systems (LDS), Granit 11 Street, Petach Tikva, Israel
[b] School of Physics and Astronomy, Tel Aviv University, Tel Aviv, Israel
[c] Bar Ilan University, Physics Department, Ramat-Gan, Israel

Available online 21 February 2008

Abstract

The Raman cross-section dependence on excitation energy in spectral range 620–248 nm have been investigated for UN, TATP, RDX, TNT, and PETN explosives. For all investigated explosive materials, significant pre-resonance enhancement in the UV spectral range has been revealed. Normalized Raman scattering signals are 100–200 times stronger with UV excitation at 248 nm compared to visible excitation at 532 nm. Thus the gated Raman technique with UV excitation has significant advantages compared to IR–VIS excitation for the remote detection of explosives. Certain of the observed Raman lines exhibit deviations from classical λ^{-4} dependence of Raman cross-section and may totally disappear with UV excitation. The possible explanation for this may be that numerous electronic transitions contribute to the molecular polarizability. These contributions could be of opposite sign and lead to partial cancellation of certain transitions. Another possible reason could be that this is a result of the stronger UV absorption that reduces the sampling volume and therefore the number of scatterers that produce the Raman signal.

1. Introduction

Raman scattering is an inelastic light-scattering process in which the frequencies of the scattered photons are shifted from those of the incident photon frequencies, according to the vibrational modes of the scattering molecule. The scattered light frequency can be of lower energy (Stokes Raman) or higher energy (Anti-Stokes Raman) than that of the incident radiation. The scattered radiation thus contains a unique set of vibrational mode frequencies for each scattering molecule. Because of its unique ability to identify molecular species, Raman spectroscopy has recently become an increasingly important tool for homeland defense (for example, see Ref. [1,2]). The technique is additionally appealing due to its remote, non-destructive and fast sensing ability. While Raman spectra are available for most explosives [3–5] only recently has this method become a promising tool for trace level detection at stand-off distances.

The main problem for Raman testing application is the weakness of Raman signals relative to Rayleigh scattering and luminescence that in many cases hide the Raman signal. Raman signal intensity may be enhanced strongly using UV excitation due to the λ^{-4} dependence of the Raman cross-section. Even much higher enhancement of the UV Raman cross-section is available in the vicinity of allowed electronic transitions [6–8]. Relatively deep UV excitation (shorter than 250 nm) also strongly diminishes the overlap of the Raman signal with luminescence due to the proximity of the Raman spectra to the excitation wavelength, which in many cases put Raman lines into the spectral range where the Stocks shifted luminescence is practically absent. When the resonance or pre-resonance condition is satisfied, not only is the Raman cross-section enhanced, the Raman spectra is also simplified since only the vibrational modes coupled to the resonant transition wavelength result in enhanced Raman cross-sections.

In spite of extensive research connected to the Raman spectra of explosive materials, there is a lack of absolute UV Raman scattering cross-sections for many of them.

* Corresponding author.
E-mail address: rosenblu@mail.biu.ac.il (M. Rosenbluh).

0925-3467/$ - see front matter © 2007 Elsevier B.V. All rights reserved.
doi:10.1016/j.optmat.2007.11.019

Here we present results of our measurements for the excitation wavelength dependence of the Raman cross-section in the spectral range of 620–248 nm for NO_3 group containing explosive Urea–Nitrate (UN) $[(NH_2)_2CO]\cdot HNO_3$, nitro (NO_2) group containing explosives cyclonite (RDX) ($C_3H_6N_6O_6$), trinitrotoluene (TNT) ($C_7H_5N_3O_6$), and pentaerythritol tetranitrate (PETN) ($C_7H_3N_3O_7$) and non-nitro-containing explosive triacetone triperoxide (TATP) ($C_9H_{18}O_6$).

2. Methodology

2.1. Theoretical analysis

The total vibrational Raman scattering cross-section σ_{mn} (in cm^2/molecule·sr) for vibrational transition $n \to m$ for an isolated molecule averaged over all its orientations is [9]

$$\sigma_{m,n}(v_0) = I_{mn}/I_0 = Cv_0(v_0 - v_{mn})3/\alpha_{m,n}(v_0)^2, \quad (1)$$

where I_{mn} is the scattered light intensity (in photons/sr·cm^2 s), I_0 and v_0 are the incident excitation beam flux (photons/s cm^2) and frequency (cm^{-1}), C is the constant, v_{mn} is the Raman vibration mode frequency (cm^{-1}) and $\alpha_{m,n}$ (v_0) is the polarizability tensor for $m \to n$ transition for the excitation frequency v_0. Eq. (1) applies to the case where the signal is obtained by counting photons over a pixel or frequency increment, as it is with most depressive/charge-coupled devices (CCD) spectrometers. If the scattered light is measured as a power rather than the number of scattered photons, one obtains $\sigma_{m,n}(v_0) \propto (v_0 - v_{mn})^4$. Classical Raman spectrometers, as well as many modern FTIR Raman spectrometers, measure power rather than photons. This consideration must be taken into account when comparing results of cross-section measurement from different sources [10]. The fourth power dependence of $\sigma_{m,n}(v_0)$ on incident frequency, v_0, means that the Raman intensity increases about 20 times when using UV laser radiation at 248 nm instead of 2nd harmonic of Nd:YAG (532 nm). An even higher increase of Raman intensity may be achieved due to the dependence of $\alpha_{m,n}$ (v_0) on excitation frequency. When the excitation frequency is nearby or approaches an electronic transition of the molecule, strong enhancement of the particular Raman vibration mode may occur and as a result strong enhancement of particular Raman lines will be observed. The pre-resonance Raman cross-section dependence on excitation frequency is described by Albrecht A-term expression [7,11]:

$$\sigma_{m,n}(v_0) = Kv_0(v_0 - v_{mn})^3\left[\frac{v_e^2 + v_0^2}{(v_e^2 - v_0^2)^2}\right]^2, \quad (2)$$

where K is a constant and v_e is the frequency of the transition to the resonant excited state. The factor $v_0(v–v_{mn})^3$ is the inherent frequency dependence of Raman cross-section and the term in parenthesis describes the frequency dependence of the polarizability $\alpha_{m,n}(v_0)$. Absolute measurements of the dependence of the Raman cross-section on excitation energy are sensitive to systematic errors due to the required absolute spectral calibration of the entire optical system. In our work we overcame this complicated task by comparing the Raman signal from the material under investigation with the Raman signal from a material with a known absolute spectrally dependent Raman cross-section, so-called Raman internal standards, used in many previous works (see for example [12–14]). As a reference signal we used the 1050 cm^{-1} Raman line (v_1 mode in [15]) of NO_3^- ions in KNO_3 powder, whose dependence on excitation wavelength was previously measured [11]. According to this method the cross-section of the investigated material $\sigma_x(\lambda)$ is determined as

$$\sigma_x(\lambda) = \sigma_{1050}(\lambda)\frac{I_x(\lambda)N_{KNO_3}}{I_{1050}(\lambda)N_x}M, \quad (3)$$

where σ_{1050} (λ) is the absolute cross-section of NO_3^- ions line at 1050 cm^{-1} at excitation wavelength λ, I_x, I_{1050} are the sample and the reference integrated Raman peak areas; N_{KNO_3} and N_x are the respective number of molecules per unit volume; M is a coefficient that can vary slightly due to difference in the Raman shift of the different materials, but due to the fact that all measured Raman lines were close to 1050 cm^{-1} this coefficient is ≈1. In certain cases (usually under near UV excitation) Raman signal was superimpose with luminescence. To get true Raman intensity the luminance spectra were approximated by polynomial curve and extracted from measured Raman spectra.

2.2. Experimental setup

Fig. 1 shows our experimental setup for Raman spectral measurements using time-gated spectroscopy, where the scattered light intensity is measured only during the laser pulse duration. The Raman spectra were excited using 5–8 ns light pulses from an Optical Parametric Oscillator (OPO) ("OPOLET" optical parametric oscillator system)

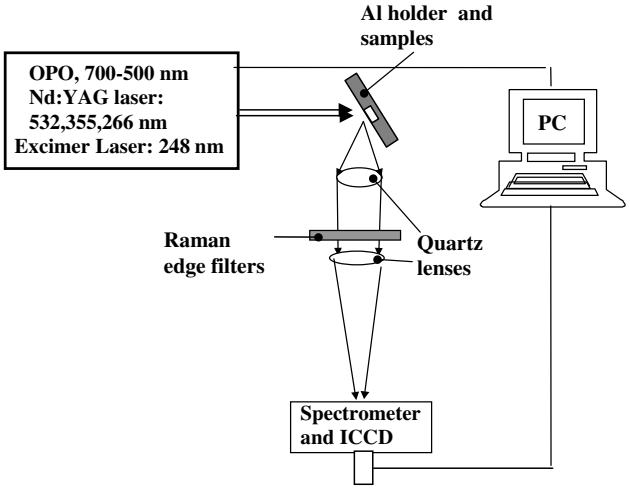

Fig. 1. Experimental setup.

for 532–632 nm excitation; from three harmonics (532, 355 and 266 nm) of a Nd:YAG flash lamp-pumped laser (Minilite II-CONTINIUM Electro-opt. Ltd); and from a KrF excimer laser with 248 nm laser pulse (PSX-501-2, NEWEKS). For UV excitation at 260–266 nm and 245–249 nm, we used a Spectra Physics MOPO HF with Frequency Doubler Option (FDO 900). To reject the strong Rayleigh scattered light, sharp-edge long pass filters (Barr Associates or Omega Optical) were placed in front of the spectrograph input. For all excitation wavelengths, the exciting light flux was held constant at about 2.5×10^{24} quanta/s cm^2 (corresponding to 0.5–1 mJ per pulse in the spectral range 248–620 nm; laser excitation area was 0.4×0.4 cm^2 on the sample region, and the pulse duration was 6×10^{-9} s). This intensity is sufficiently small so as to prevent the measurable effect of the photodecomposition of the samples under UV excitation. Light at the output of the spectrometer (Oriel Instruments 260i) was detected by a time gated ICCD device (Andor, iStar). The spectral resolution was ~10 cm^{-1}. We used a minimal accumulation number of Raman scattered pulses (20–50) as an additional precaution for preventing significant photodegradation of the measured samples.

2.3. Samples

An aluminum (Al) plate with a 1 mm deep indentation of 1 mm diameter was used as the sample holder. Al was chosen as the substrate due to its very low luminescence in all spectral regions used in our experiments. The Al holder was placed at an angle with respect to the excitation beam so as to prevent direct reflectance of the excitation laser light to the spectrometer. The indentation in the holder was filled with a highly dispersed powder of the explosive under study, and due to the small differences in volume densities of the investigated explosives [16], the number of molecules per unit volume remained constant for all investigated explosives. Furthermore, the N_{KNO_3}/N_x ratio in Eq. (3) was approximately equal to 1 in the experiments. The samples and reference were placed sequentially into the Al plate holder that was fixed at the same position relative to the excitation light and Raman signal collection system, which allowed us to avoid any geometrical corrections in measuring the Raman intensities from different materials.

3. Results and discussion

3.1. NO_3^- ions

As was previously described, we used the KNO_3 Raman spectra as the reference for the measurement of the absolute cross-section for explosives. Fig. 2 shows the Raman spectra of NO_3^- ions (KNO_3 crystalline powder) for 532 and 355 nm (Fig. 2a) and for 266 and 248 nm (Fig. 2b) excitation wavelengths. All spectral intensities are given in arbitrary units, but the relative intensities are as indicated. The lines at 714, 1050 and 1354 cm^{-1}, which are observed under 625, 532 and 355 nm excitations, are attributed to internal covalent vibrations of the NO_3^- ions [17,15]. Under deep UV excitation, a series of Raman lines at higher energies appear at approximately regular intervals (about 340 cm^{-1}). We suppose that these nearly equally spaced lines are the fundamental vibration mode at 1050 cm^{-1} and its overtone lines at 1355, 1669, 2100, 2431, 2757, and 3102 cm^{-1}. Fig. 3 demonstrates dependence of the cross-section for the most intensive line, 1050 cm^{-1}, on the excitation energy measured by Dudik

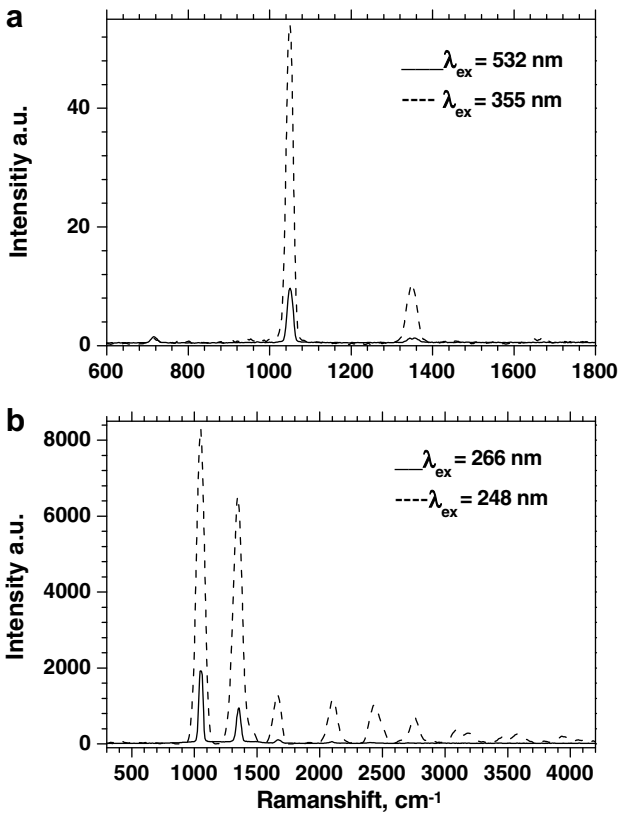

Fig. 2. Raman spectra of KNO_3: (a) 532 and 355 nm excitations; (b) 266 and 248 nm excitations.

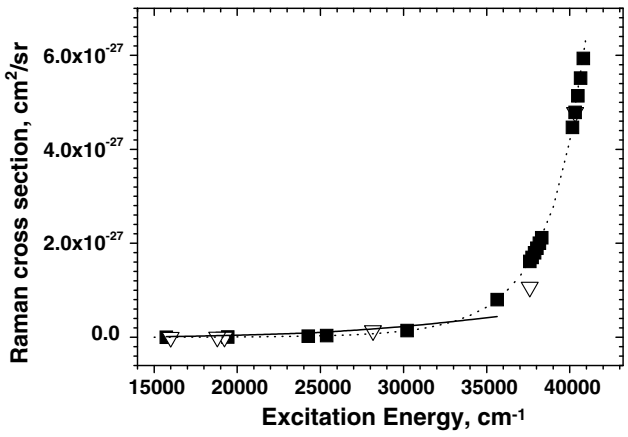

Fig. 3. Raman cross-section of NO_3^- 1050 cm^{-1} line as a function of excitation wavelength. ■ – Dudik data for 1045 cm^{-1}, ▽ - our experimental data, dot line – best fit by Eq. (3), solid line – best fit by Eq. (1).

et al. [11] (squares) and by us (triangles). In the common spectral range, where comparison is possible, our data coincides well (up to a constant) with Dudik's et al. data. The solid line is a best fit of the data (ours and that taken from Ref. [11]) to a $\nu(\nu_0-\nu_{mn})^3$ dependence. The dotted line is a best fit of the experimental data, enabling calculation of the absolute cross-section using the pre-resonance A term. These cross-sections for the 1050 cm^{-1} line for NO_3^--ions are used as internal Raman standard in our experiments.

3.2. Urea nitrate

Urea nitrate (UN) is a 1:1 compound of urea $(NH_2)_2CO^-$ and nitric acid HNO_3, with a formula of $[(NH_2)_2CO]\cdot HNO_3$ is an NO_3-containing material. It is widely used in the manufacture of fertilizers, but is also known as an easily synthesized homemade explosive, which was used, for example, in the 1993 explosion of the NY World Trade Center. Fig. 4 shows the UN Raman spectra for different excitation wavelengths, while the Raman spectra of urea are also shown for comparison. The most intense line in UN (1050 cm^{-1}) coincides with the 1050 cm^{-1} line of KNO_3 and is attributed to symmetrical stretching vibration of NO_3^- ion. In pure urea the most intensive line is situated at 1010 cm^{-1}. It is also seen in the UN Raman spectra for 625 and 532 nm excitations and was assigned to the CN symmetric stretching mode of urea molecule [18,19]. Raman lines that are attributed to pure urea almost disappear in UN spectra with increasing excitation energy and a series of lines at higher Raman shift appear, very similar to those observed for NO_3^- molecule in KNO_3 vibration spectra (Fig. 5). Fig. 6 shows our estimations for the spectral dependence of the absolute cross-sections of the 1050 cm^{-1} line in UN (squares) and for the 1010 cm^{-1} line in pure urea (circles). The line at 1050 cm^{-1} in UN demonstrates quite different dependence on excitation energy compared to the line at 1010 cm^{-1} in UN and in urea. The spectral dependence of the cross-section of the line at 1050 cm^{-1} reveals a small maximum at about 40,600 cm^{-1} (see inserts in Fig. 6) and may be well approximated by the pre-resonance Albrecht A-term with resonant frequency ν_0 of 48,500 cm^{-1} (about 200 nm) (Eq. (2)). This wavelength is close to the 200 nm absorption band in UN [20,21] and is assigned to the $\pi \rightarrow \pi$ transition of nitrate. The line at 1010 cm^{-1}, on the other hand, varies almost exactly as $\nu(\nu_0-\nu_{mn})^3$ revealing complete lack of pre-resonance enhancement. This strong difference in excitation energy dependence is due to the fact that these Raman lines in UN are derived from different electronic transitions.

3.3. RDX

RDX is a widely used military explosive containing a nitro group (NO_2). Fig. 7 shows the Raman spectra of RDX under excitation in the spectral range of 266–625 nm. Our results

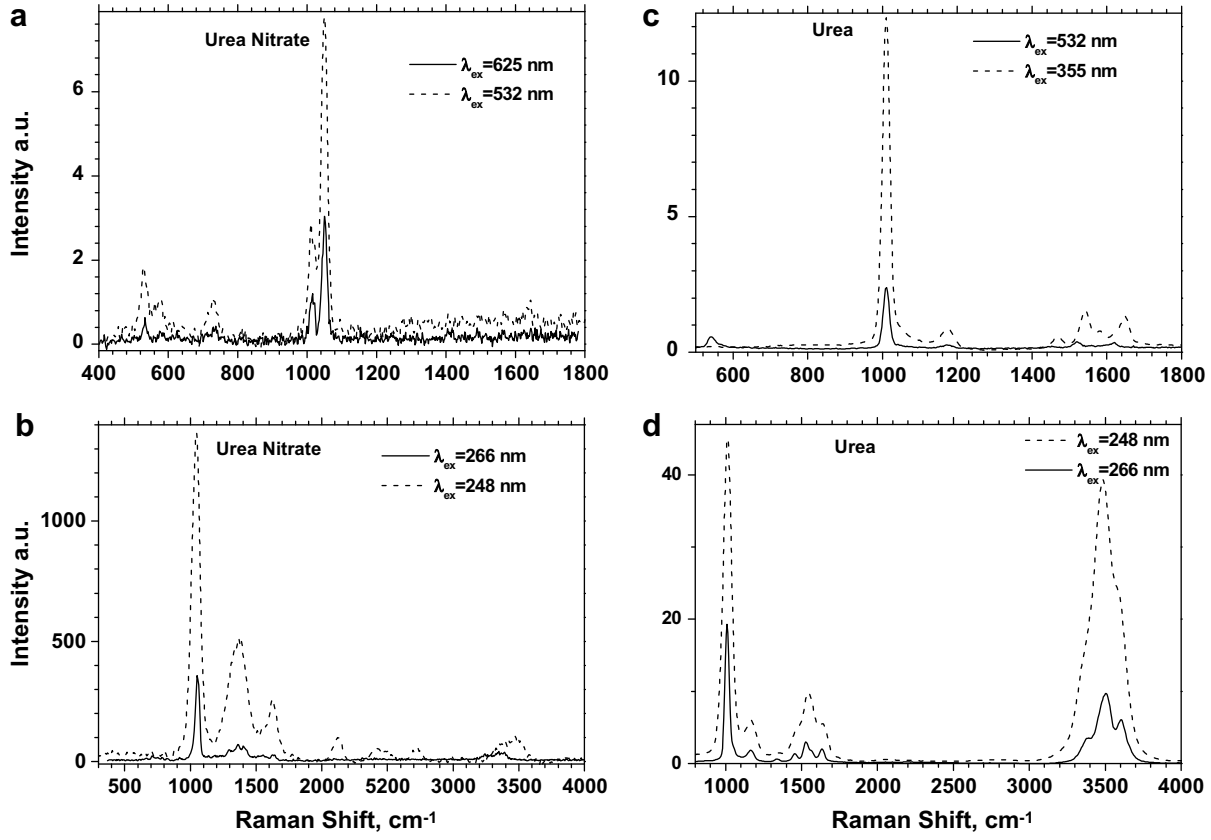

Fig. 4. Raman spectra of: Urea Nitrate (a,b); Urea (c,d).

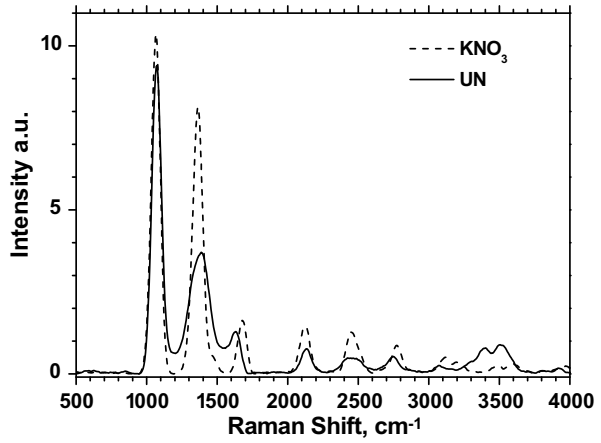

Fig. 5. Raman spectra of Urea Nitrate and KNO_3 under excitation by 248 nm.

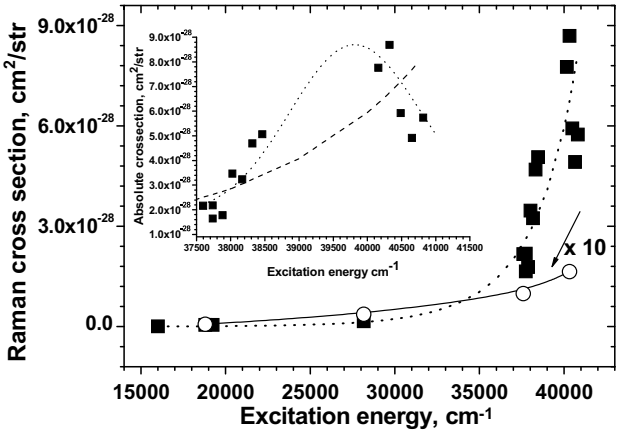

Fig. 6. Calculated cross-sections for the lines at 1050 cm^{-1} in Urea Nitrate (squares) and 1010 cm^{-1} in Urea (circles). Insert – the spectral dependence of the cross section of the line at 1050 cm^{-1} with a maximum at about 40,600 cm^{-1}.

for visible-near UV excitation (Fig. 7a) coincide well with data in the literature obtained under similar conditions [3]. The spectra of RDX dramatically change when moving to deep UV excitation. The well-known narrow lines in the spectral range of 500–1700 cm^{-1} and in the vicinity of 3000 cm^{-1} disappear completely. Instead a relatively broad, poorly resolved double band appears in the spectral range of 1500 cm^{-1} (Fig. 7b). The line at 887 cm^{-1}, which is the most intense feature for excitation in spectral range of 355–625 nm, may be attributed to ν(C–N–C) ring vibrations [4]. The measured dependence of the cross-section of this line in the spectral range of 355–625 nm is presented in Fig. 8(squares). The fit of the data to the $\nu(\nu_0-\nu_{mn})^3$ dependence (solid line) is not satisfactory and reveals the pre-resonance enhancement of this mode. Much better fit may be achieved using the pre-resonance Albreht A-term (Eq. (2)) with resonance frequency $\nu_e \sim 10^5$ cm^{-1} (100 nm) (dotted line in Fig. 8), but this resonance frequency is too far in the UV. From the dramatic drop in Raman intensity for excitation by wavelengths shorter than 355 nm it is obvious that the resonance frequency associated with the line at 887 cm^{-1} must be in the spectral range of 266–355 nm.

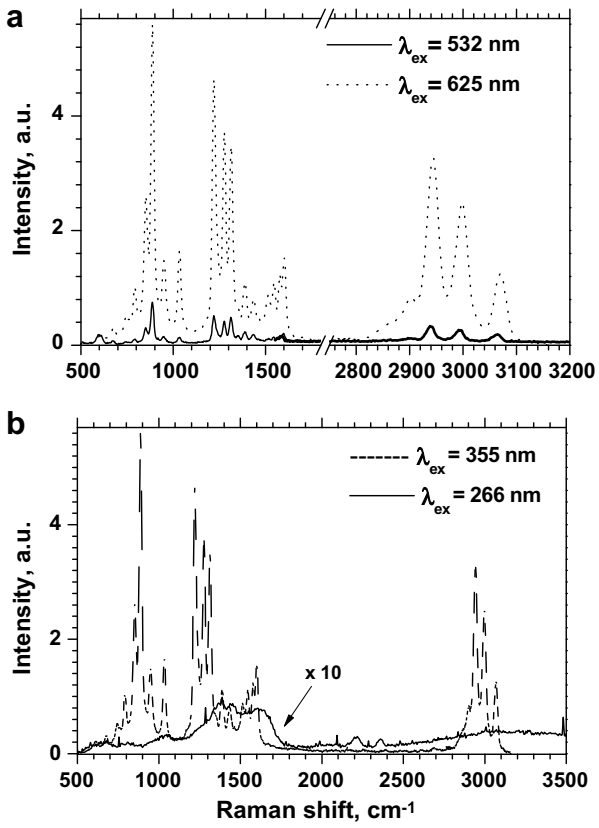

Fig. 7. Raman spectra of RDX: (a) 532 and 355 nm excitations; (b) 355 and 266 nm excitations. Raman spectrum with 355 nm excitation presented on both (a) and (b) graphs for comparison sake.

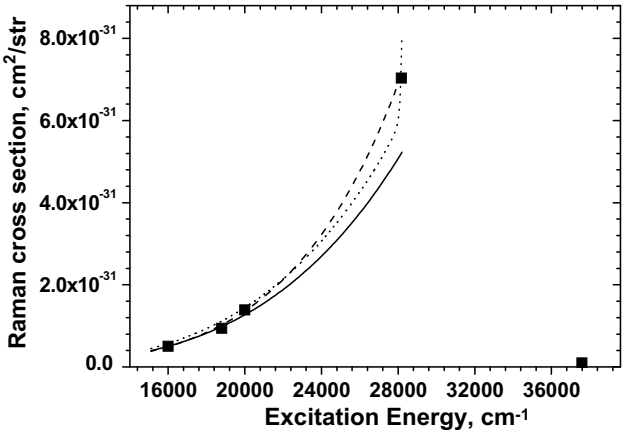

Fig. 8. Raman cross-section dependence on the excitation energy for the line at 887 cm^{-1} of RDX. ■ – our experimental data, solid line – best fit by Eq. (1), dot line – best fit by Eq. (4), dash line –best fit by Eq. (2).

The fact that the Raman line at 887 cm^{-1} for UV excitation at 266 nm is much weaker than the Raman intensity for the same line excited by 532 nm, contradicts the classical λ^{-4} dependence of the Raman cross-section. A possible explanation may be that the A-term approximation assumes that

only one electronic transition dominates the Raman resonance enhancement, but in actuality numerous transitions contribute to the molecular polarizability [7]. The relative contributions will be excitation-wavelength dependent and could be of opposite sign at certain excitation wavelengths, leading to partial cancellation of the molecular polarizability. If our hypothesis is correct, the A-term fit may result in an overestimation of the resonance transition energy for the closest-lying state contributing to the Raman scattering. A simplest phenomenological model, which takes into account the higher-lying, excited states that contribute to molecule polarizability, can be proposed as [7,9,13]:

$$\sigma_{m,n}(v_0) = K_3 v(v_0 - v_{mn})^3 \left[\frac{v_e^2 + v_0^2}{(v_e^2 - v_0^2)^2} + K_4\right]^2, \quad (4)$$

where K_3, K_4 are constants. The best fit of the RDX experimental data by such expression (dotted line in Fig. 8) gave a resonance frequency of $v_e = 28{,}500\ cm^{-1}$ (350 nm). This frequency is in good coincidence with the reported [22] 345 nm strong absorption band of RDX. This may qualitatively explain the Raman intensity dependence on excitation energy in spectral range up to 28,985 cm^{-1} (355 nm), but much more experimental data is necessary in the direct vicinity of this maximum for better understanding of the phenomena.

Another possible reason for drastic reducing of Raman signal intensity under excitation at wavelengths shorter than 355 nm may be the strong UV absorption in the vicinity of 345 nm [22] that reduces the sampling volume and, therefore, the number of scatterers that produce the Raman signal.

3.4. TNT

Trinitrotoluene ($C_7H_5N_3O_6$) is another example of an NO_2-containing explosive. The Raman spectrum under 532 nm excitation (Fig. 9a) is very similar to spectra obtained by other authors under excitation in the spectral range of 633–1064 nm [4,23]. In the spectral range of 500–3200 cm^{-1}, twelve Raman lines are observed with the most intense at 794, 825, 1229, 1360, 1554, 1635 and 2968 cm^{-1}. They are attributed to CH stretches, NO_2 symmetric and anti-symmetric and CH_3 symmetric and anti-symmetric stretches. Under deep UV excitations (266 and 248 nm) the Raman spectrum of TNT changes: lines at 1359, 1609, 2780 and 3096 cm^{-1} appear (Fig. 9b). This behavior is similar to that reported [24] under 244 nm excitation, with the only exception that the lines in the vicinity of 3000 cm^{-1} have a much higher relative intensity. The Raman spectra change from visible to UV excitation may be explained by the fact that TNT possess two strong electronic absorption bands in the vicinity of 420 nm and 220–250 nm [24], and two sets of detected Raman lines are derived from these two electronic transitions.

The estimated cross-section dependence on excitation energy for the most intense line at 1360 cm^{-1} (NO_2 symmetric stretch [4]), shown in Fig. 10, reveals the strong pre-resonance enhancement of this mode. The resonance frequency derived from this approximation is about $6.8 \times 10^4\ cm^{-1}$ (150 nm), which is higher than the reported [24] absorption maximum. The fitting of the experimental data by an expression like Eq. (4) gave a more realistic resonance frequency of $v_e = 5.35 \times 10^4\ cm^{-1}$ (190 nm), but the theoretical base of this approximation must be clarified. Estimated parameters for this line are given in Table 1 for

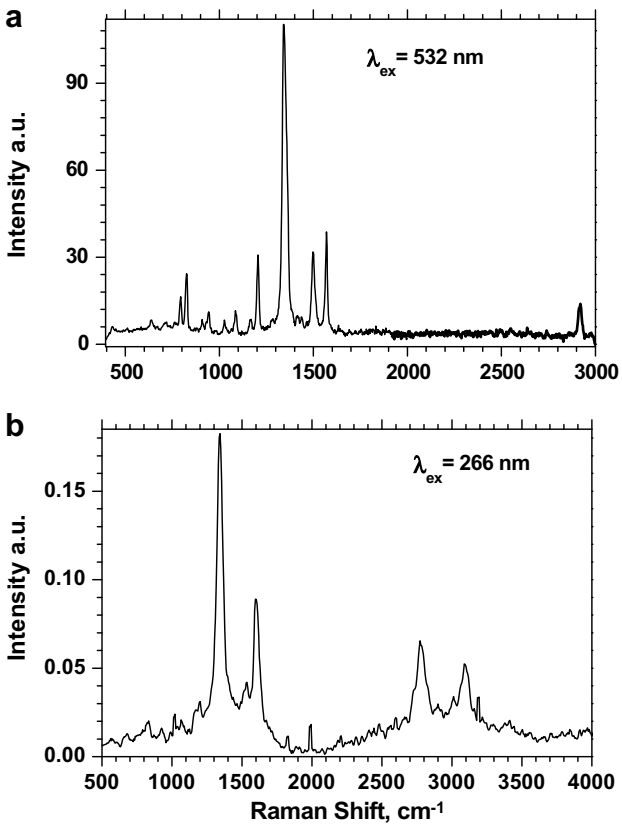

Fig. 9. Raman spectra of TNT: (a) 532 nm excitation and (b) 266 nm excitation.

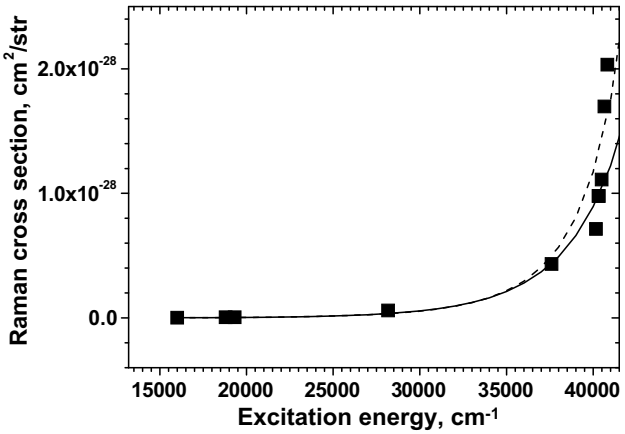

Fig. 10. Raman cross-section dependence on the excitation energy for 1340 cm^{-1} line in TNT. Solid line – best fit by Eq. (3), dash line – best fit Eq. (4).

Table 1
Parameters for the Albrecht A term fits (Eq. (3)) for investigated explosives

Material (line cm^{-1})	K (cm^2)	ν_e (cm^{-1})	λ_e (nm)
KNO_3 (1050)	1.56×10^{-28}	5.23×10^4	190
UN (1050)	3.4×10^{-29}	4.8×10^4	210
RDX-5 (890)	7.6×10^{-29}	1.1×10^5	90
TNT (1340)	1.8×10^{-29}	$5.9 \times 1\ 0^4$	170
PETN (1280)	6.5×10^{-27}	1.5×10^5	66
TETP(2290)	1.67×10^{-28}	7.28×10^4	137

A-term approximation and in Table 2 for modified A-term approximation.

3.5. PETN

PETN is another example of nitro group (NO_2)-containing explosive; its Raman spectra under excitations of 520 and 248 nm are shown in Fig. 11. The Raman spectra of PETN also change with excitation wavelength, but not as dramatically as was observed for TNT. The Raman spectra of PETN under visible laser excitation (520–625 nm) consist of sharp lines attributed mostly to CH-ring bends, to CN stretches and to symmetric and anti-symmetric stretches of CH_3. The intense line at 1287 cm^{-1} and weak line at 1654 cm^{-1} are due to symmetric and anti-symmetric stretches of the NO_2 molecule, respectively. Under UV excitation the Raman spectra become much simpler, with only an ON stretching mode at 870 cm^{-1}[4], symmetric and anti-symmetric stretching of NO_2 modes at 1287 cm^{-1} and 1655 cm^{-1} and a broad unresolved band at 3060 cm^{-1} connected to the CH_3 stretches. In addition, the Raman lines become much broader. The absolute cross-section dependence on excitation energy of the line at 1287 cm^{-1} is shown in Fig. 12 (squares). The Raman cross-section at 1290 cm^{-1}, for excitation wavelengths up to 266 nm, can be fit equally well with a $\nu(\nu_0-\nu_{mn})^3$ dependence (dashed curve) or a pre-resonance Albreht A-term expression (dotted curve).

Table 2
Estimated parameters derived from best fit to Eq. (4)

Material (line cm^{-1})	λ_e (nm)	ν_e (cm^{-1})	K_3	K_2
RDX (890)	350	2.83×10^4	3×10^{-5}	$1.5\ 10^{-41}$
TNT (1340)	190	5.35×10^4	3.5×10^{-8}	3.9×10^{-30}
PETN (1280)	230	4.22×10^4	9.5×10^{-7}	2.0×10^{-35}
TATP (2990)	172	5.87×10^4	9.0×10^{-10}	7.0×10^{-29}

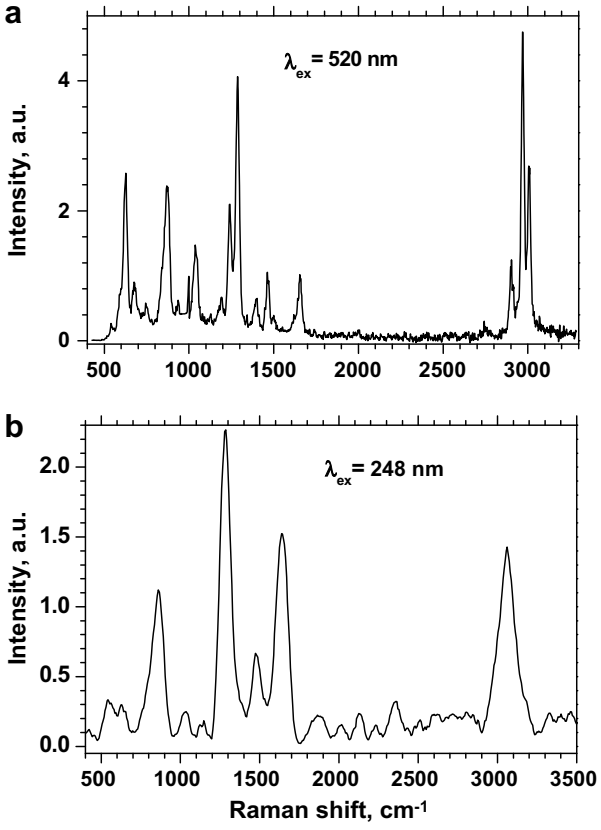

Fig. 11. Raman spectra of PETN: (a) 520 nm excitation and (b) 248 nm excitation.

3.6. TATP

Most conventional high explosives contain nitro groups, but some improvised explosives contain no nitrogen at all; rather, they are based on organic peroxides. One of these peroxide-based explosive compounds is TATP (Triacetone triperoxide). These explosives can be manufactured cheaply and relatively easily at home from off-the-shelf ingredients, but despite their simple nature peroxide-based explosives are highly lethal.

Fig. 13 represents the Raman spectra of TATP under 500 and 248 nm excitations. Similar to the other explosives, under deep UV excitation the Raman spectra are simpler compared to visible excitation. Instead of eight Raman lines detected under visible excitation in spectral range of 300–3000 cm^{-1}, only two unresolved intense bands remain the first at 860–940 cm^{-1}, that may be attributed to C–N–C

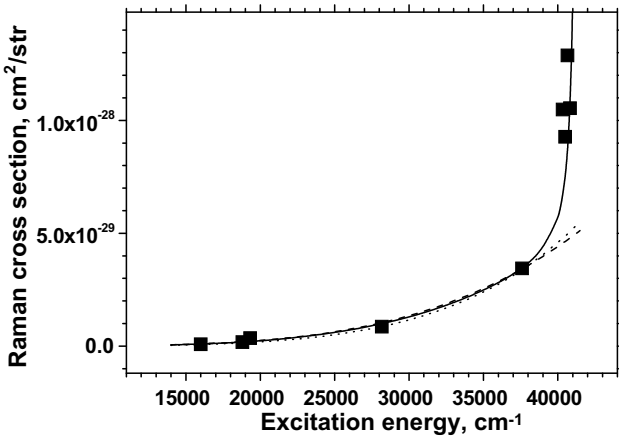

Fig. 12. Raman cross-section dependence on the excitation energy for the line at 1290 cm^{-1} of PETN. Solid line – best fit by Eq. (4) ($\nu_e = 41800\ cm^{-1}$), dot line – best fit by Eq. (3) ($\nu_e = 1500000\ cm^{-1}$), dash line – best fit by Eq. (1).

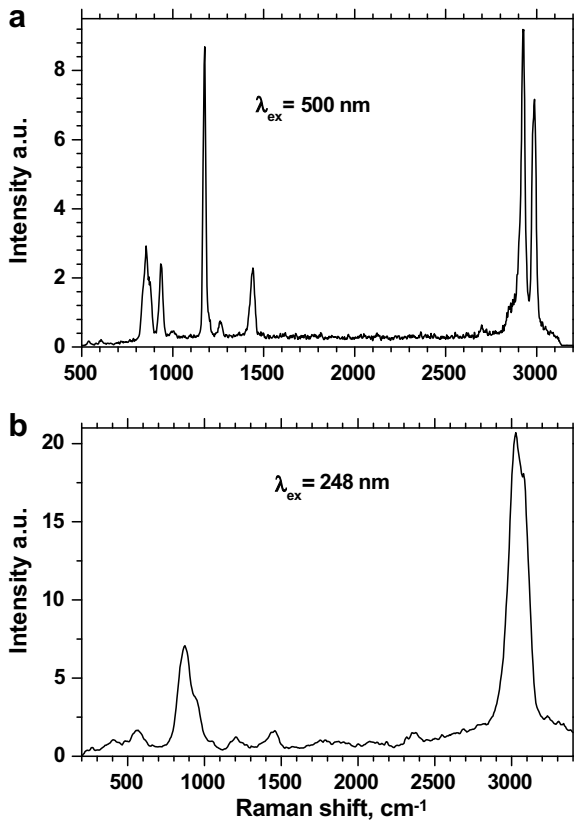

Fig. 13. Raman spectra of TATP: (a) 520 nm excitation and (b) 248 nm excitation.

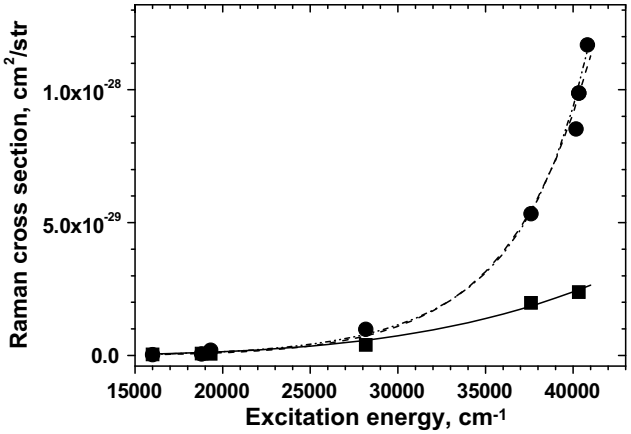

Fig. 14. Raman cross-section of the lines at 890 cm^{-1} (squares) and 2990 cm^{-1} (circles) in TATP. The solid line is approximation to $v(v_0-v_{mn})^3$ dependence for the 890 cm^{-1} line, the dotted line is A-term approximation of the line at 2990 cm^{-1} and the dashed line is empirical approximation by Eq. (4) (the last two lines practically coincide, but yield different approximation parameters).

and C–H ring vibrations, and the second in the spectral range near 3000 cm^{-1}, that may be attributed to CH_3 stretches. Fig. 14 demonstrates the dependences of the cross-sections of these two groups of lines on excitation energy. It may be seen that the lines at 860–940 cm^{-1} obey to $v(v_0-v_{mn})^3$ dependence demonstrating the absence of pre-resonance enhancement, while the line in vicinity of 3000 cm^{-1} exhibits strong pre-resonance enhancement. The best-fit parameters of absolute cross-section dependence on excitation energy are given in Table 1 for Eq. (2) and in Table 2 for Eq. (4).

4. Conclusions

The results of the present investigation demonstrate that UV excitation of Raman scattering can have significant advantages over visible excitation for the remote detection of explosives. The dependence of the Raman cross-section on excitation energy reveal significant pre-resonance enhancement of certain Raman lines in the UV spectral range for most investigated explosives. It was found that some of the Raman lines exhibit deviations from classical λ^{-4} dependence of Raman cross-section and may totally disappear with UV excitation. The possible reason is that different Raman lines derive from different electronic transitions and disappear when the excitation energy exceeds the corresponding resonance energy. The results of our investigation will allow the determination of the optimal excitation source and the evaluation of the necessary parameters for the construction of a Raman LIDAR.

References

[1] J. Steinfeld, J. Wormhoudt, Annu. Rev. Phys. Chem. 49 (1998) 203.
[2] D. Moor, Rev. Sci. Instr. 75 (2004) 2449.
[3] S. Lewis, N. Daniel, N. Chaffin, P.Griffith, M. Tungol, Spectrochem. Acta Part A 51 (1995) 1985.
[4] I. Lewis, N. Daniel, P. Griffith, Appl. Spectrosc. 51 (1997) 1854.
[5] C. Cheng, T. Kirkbride, D. Batchelder, R. Lacey, T. Sheldon, J. Forensic Sci. 40 (1995) 31.
[6] W. Keifer, in: B. Schrader (Ed.), Infrared and Raman Spectroscopy, vch, Weinheim, 1995.
[7] A. Albrecht, M. Hutley, J. Chem. Phys. 55 (1971) 4438.
[8] S. Asher, Annu. Rev. Phys. Chem. 39 (1988) 537.
[9] J. Tang, A. Albrecht, in: H. Szymanski (Ed.), Raman Spectroscopy, vol. 2, Plenum, NY, 1970 (Chapter 2).
[10] R. McCreery, Photometric standards for Raman spectroscopy, in: J. Chalmers, P. Giffiths (Eds.), Handbook of Vibration spectroscopy, J. Wiley & Sons, 2002, p. 1.
[11] J. Dudik, C. Jonson, S. Asher, J. Chem. Phys. 82 (1985) 1732.
[12] J. Nesor, E. Lippincott, J. Raman Spectrosc. 1 (1973) 305.
[13] D. Blazej, W. Peticolas, J. Chem. Phys. 72 (1980) 3134.
[14] S. Christesen, Appl. Spectrosc. 42 (1988) 318.
[15] D. Liu, F. Ulman, J. Hardy, Phys. Rev. B 45 (1992) 2142.
[16] J. Yinon, Forensic and Environmental Detection of Explosives, John Wiley & Sons Ltd.,, 1999.
[17] M. Balkanski, M. Teng, N. Nusimovici, Phys. Rev. 3 (1968) 1099.
[18] X. Hoccart, G. Turell, J. Chem. Phys. 99 (1993) 8498.
[19] N. Wen, M. Brooker, J. Chem. Phys. 97 (1993) 8608.
[20] S. Sander, J. Phys. Chem. 90 (1986) 4135.
[21] T. Chen, S. Xiao, P. Li, Int. J. Quant. Chem. 64 (1997) 247.
[22] Von H. Whitlel, AIP Conf. Proc. 845 (2006) 1357.
[23] H. Sands, I. Hayward, T. Kirkbride, R Bannett, R. Lacey, D. Batchelder, J. Forensic Sci. 43 (1997) 509.
[24] R. Hummel, A. Fuller, C. Schollern, P. Holloway, Detection of explosives materials by differential reflection spectroscopy, Appl. Phys. Lett. 88 (2006), 231903-1-3.